Application Note 49

Theory of Lloyd's Mirror Interferometer

Newport Corporation

Newport®
Experience | Solutions

INTRODUCTION

There are two principal methods for producing coherent sources for interferometry. One uses the division of wavefront, as in the Young's double slit experiment. The second divides the amplitude between two arms, as in the Michelson interferometer. The Lloyd's Mirror approach uses wavefront division at a mirror to produce two-source interference patterns. The basic setup is shown in Figure 1. This was first described by English physicist Humphrey Lloyd in 1834.

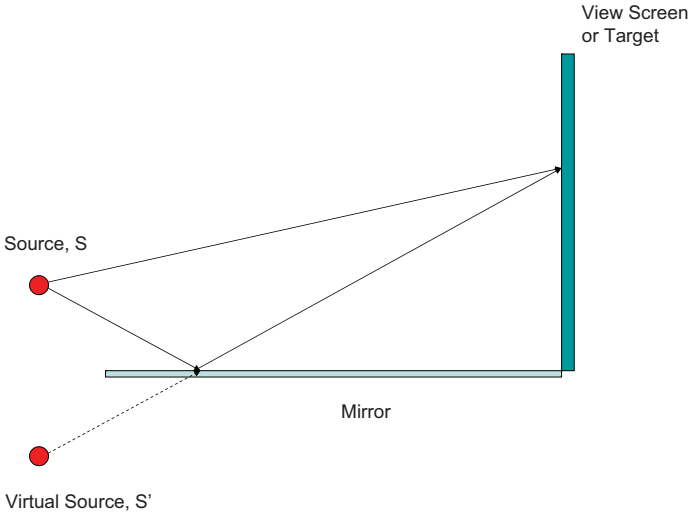

Figure 1

A source, S, emits coherent light into a cone such that some of the light follows a path that goes directly to the target while light emitted at a higher angle reflects from the mirror and upon reflection also goes to the target. The light reflected from the mirror then appears to have come from a virtual source, S'. When the light from the two paths is in phase a bright fringe appears and when the light is out of phase a dark fringe appears at the target.

THEORY OF THE LLOYD'S MIRROR INTERFEROMETER

The two sources, real (S) and virtual (S'), become analogs for the two slits in Young's double-slit experiment. In 1801, Young demonstrated the interference of light, thereby establishing its wave nature. In 1803, he presented a paper to the Royal Society demonstrating two-slit diffraction. Young's original sketch, based on his observation of water waves, is shown in figure 2. He showed that the pattern formed by light at an observation screen is exactly analogous to the pattern shown for water waves.

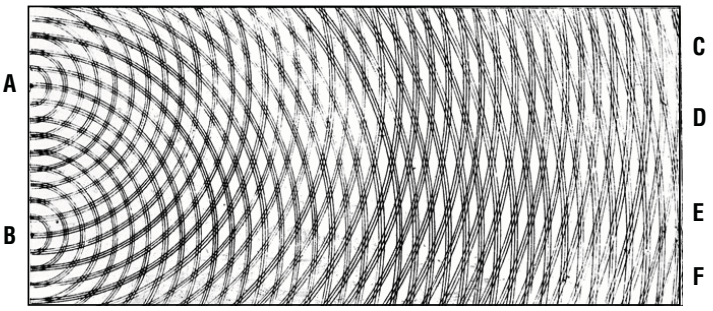

Figure 2

Now it's time to do the math. We need to derive an expression for the intensity of the light at any point on the observation screen. The theory that we have here is very similar to the theory for Young's double-slit interference, which you can find in many standard optics texts, such as Jenkins and White[1] or Hecht.[2] We start with two waves of light emerging from our real source S and appearing to emerge from our virtual source S', separated by a distance d, which we assume to be small. Figure 3 is a repeat of Figure 1, but with more detail for the development of the theory.

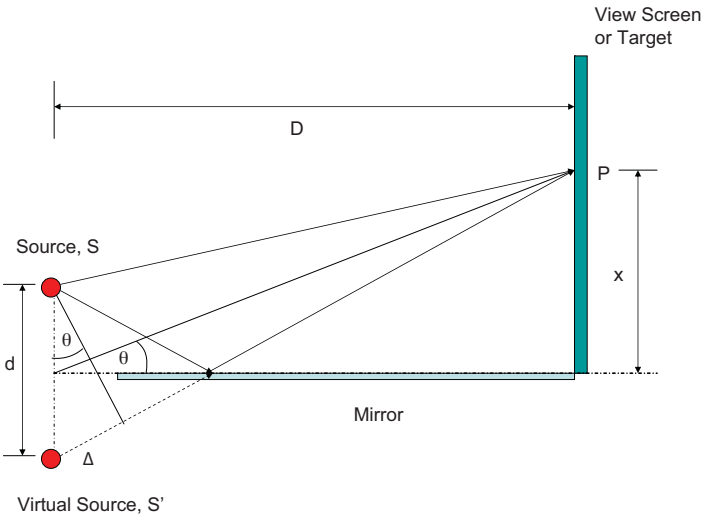

Figure 3

The distance from the sources to the screen is D. The two waves are superimposed on the screen at a point P at some distance, x, from the center line, which is defined by the center between the two sources, which in turn is the plane of the mirror. The intensity at P is determined by the phase difference between the two waves, and that phase difference is related to the path length difference, Δ. The angle θ is equal to x/D, but that is also equal to Δ/d, by reference to similar triangles. The phase difference will be the wavenumber times the path length difference. However, in the Lloyd's mirror, there is an extra phase shift of π at the reflection from the mirror surface that we would not have in Young's double-slit, which we must take into account in our calculations. That phase difference, explicitly including the extra phase shift of π upon reflection, is then:

$$\delta = k\Delta = \frac{2\pi}{\lambda} d \sin\theta - \pi$$

The intensity at the point P will be the square of the amplitude, A, which is the sum of that contributed by the two beams, each with amplitude a.

$$I = A^2 = 2a^2\,(1+\cos\delta) = 4a^2\cos^2\left(\frac{\delta}{2}\right)$$

We can write δ as:

$$\delta = \frac{2\pi}{\lambda}\, d\, \frac{x}{D} - \pi$$

So, we will have bright fringes when:

$$x = (m+{}^1\!/_2)\,\lambda\,\frac{D}{d}$$

We have a bright fringe for any integer, m, meeting this condition. This development is for the two-dimensional case, analogous to Young's experiment, where we only consider the phase shift in the plane, resulting in a one-dimensional line for the fringe pattern. The theory can be extended to three dimensions to give us a two-dimensional pattern on the screen. That is beyond the scope of this Application Note, but the development of the theory in three dimensions to yield a two degree-of-freedom Lloyd's Mirror interferometer pattern can be found in Reference 3.

In this development of the theory, we have not made any assumption about the intensity of light from each source. Because the virtual source at S' is due to a reflection in a mirror, the intensities from the two sources will not be the same. If the intensity from S is equal to I_1, then the intensity from the virtual source S' will be $I_2 = R \times I_1$, where R is the reflectivity of the mirror. Since we are dealing with two sources that are ideally monochromatic point sources, the predicted visibility is.[4,5,6]

$$\text{Visibility (ideal)} = \frac{2\sqrt{I_1 I_2}}{I_1+I_2}$$

In practice, even with, for example, an aluminum mirror with R ~ 80% in the UV, the loss of visibility will be small and the visibility would be approximately 99% of the ideal maximum. However, the spectral range employed may in some cases restrict the reflectivity that can be realized, and thereby the visibility that can be achieved, using commercially-available mirrors.

POWER OF THE TECHNIQUE

Let's go back and look again at Figure 3. If we move the source S farther from the mirror (that is, up in the figure), we see that the virtual second source S' also moves farther from the mirror (down in the figure). So, the distance d is increased by an amount that is two times the distance that S has been moved. From our equation for the positions of the bright fringes, we see that increasing d reduces the distance between those bright fringes. As d increases we can produce finer and finer features in the interference pattern.

If we increase d in a standard double-slit interference, we also have to expand the input beam so that it covers both slits. This results in a large loss of power since all the light incident on the barrier between the two slits is lost. However, using the Lloyd's mirror technique, increasing d does not result in additional power loss since the second "slit" is just the virtual image of the source in the mirror. Therefore, the Lloyd's mirror technique is powerful in that we can achieve very small details in the interference pattern while maintaining the power level that is needed for applications that require high light levels, such as photolithography.

One of principal advantages of the Lloyd's mirror technique is its simplicity. The increase or decrease of the separation d can be simply achieved by rotating the system of mirror and target with respect to the laser source. Once the laser and its focusing optics are in place, they do not need to be changed to control the pattern formed at the target. Only one degree of control, the adjustment of a rotation stage, is all that is required. We will look at that in more detail in a later section (Equipment) of this note.

APPLICATIONS:

INTERFERENCE LITHOGRAPHY

The most common current application of the Lloyd's mirror technique is in UV photolithography and nanopatterning. This interference lithography (IL) technique has been used to create periodic nanoscale patterns on relatively large substrates. [3 and references therein] This lithographic technique relies on constructive and destructive interference to write a pattern in a photoresist film. Surface patterning using IL has been shown to increase the incident light in absorber layers of GaAs.[7]

Improvement of the biofunctionality in implants using nanofeatures generated by IL has been explored in titanium implants.[8] The IL technique using a Lloyd's mirror has also been used to write directly in alkylphosphonates adsorbed on oxides of titanium to produce nanostructured polymer monolyaers.[9]

Although this work is usually done in the UV portion of the spectrum, the Lloyd's mirror IL technique has been extended to the visible at 405 nm,[10] and to the extreme UV at 46.9 nm.[11]

OTHER APPLICATIONS

While interference lithography is the most common application, the Lloyd's mirror interferometer has been used in a wide range of applications. A sampling of these applications includes:

- Direct measurement of MTF (modulation transfer function) of CCD's.[12]
- Manufacturing of Fiber Bragg gratings using phase plates.[13]
- Laser diode beam shaping.[14]
- Compact Fourier transform wavemeter for pulsed lasers.[15]
- Laser-plasma diagnostics (in the extreme UV).[16]

EQUIPMENT

As described above, most applications of the Lloyd's mirror make use of a UV laser. The optical components chosen in the list shown here are intended for use with a HeCd laser at 325 nm or a tripled (355 nm) or quadrupled (266 nm) Nd:YAG laser. Two basic options for the experiment are illustrated schematically in Figure 4; Figure 4a showing the setup with a collimating lens and Figure 4b showing the setup without a collimating lens. The trade-offs associated with these two versions of the system are discussed below at the collimating lens assembly.

Spatial filter assembly:

For an in-depth discussion of spatial filtering, please refer to the Technical Note, Spatial Filters, at our website, www.newport.com/Spatial-Filters/144910/1033/content.aspx.

- 910A
- U-27X
- 910PH-5
- SP-3
- VPH-3-P
- PS-F

Collimating lens assembly:

This collimating lens may be eliminated if the experiment requires expansion of the beam to a large diameter. If the target has a small area, the version in Figure 4a using a collimating lens will result in a higher power density per unit area of the target. A large beam diameter will be achieved using the setup without the collimating lens in Figure 4b. This allows wider coverage but will also reduce the power density per unit area requiring longer exposure times.

- SPX055AR.10 (f = 300 mm)
- LH-1
- SP-3
- VPH-4-P
- PS-F

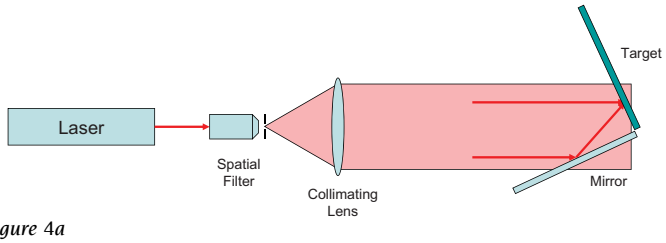

Figure 4a

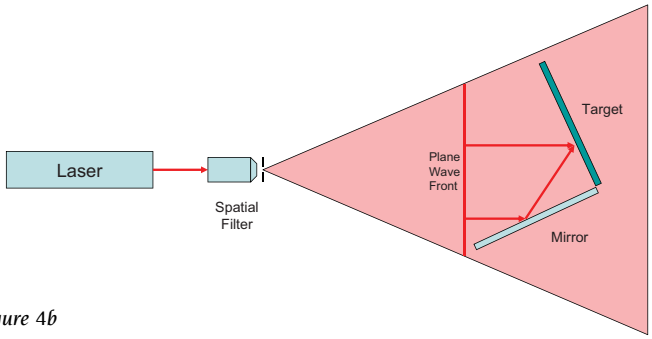

Figure 4b

Lloyd's mirror interferometer assembly:

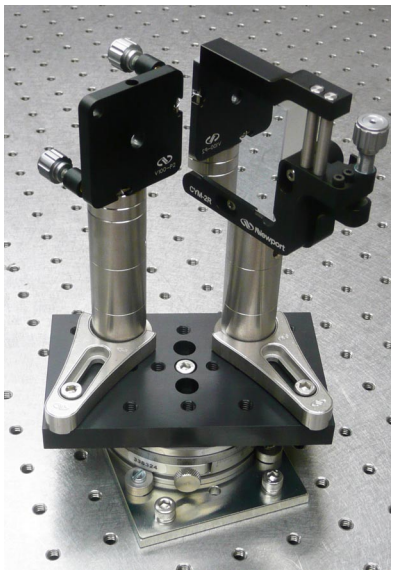

20SD520AL.2

(The mirror included here is a 2" square UV-enhanced aluminum mirror. This mirror is designed for use in the UV portion of the spectrum and has a large area that is useful in UV lithographic nanopattern applications.)

- V100-P2
- 2x PS-3
- 2x PS-0.25
- UTR80S
- CYM-2R
- 2x PS-F
- 38
- M-PBN8

Mirror assembly (2x):

This mirror assembly for steering the beam from the laser to the interferometer is optional, depending upon the space requirements of the experimental setup on the optical table.

- 10D20RM.2
- SP-3
- PS-F
- U100-A2K
- VPH-4-P

ACKNOWLEDGMENT

Newport Corporation wishes to acknowledge and thank Mr. Ishan Wathuthanthri, Stevens Institute of Technology, Mechanical Engineering Department, Hoboken, NJ, for his consultation, criticism, and kind assistance in the preparation of this application note.

NOTES

The references cited in this list provide a background for understanding the Lloyd's mirror interferometer. The references included here present a sampling of the literature that is available, but this list is not intended to be an exhaustive survey of published research.

1. Francis A. Jenkins and Harvey E. White, F*undamentals of* O*ptics*, chapter 13, McGraw-Hill.
2. Eugene Hecht, Optics, section 9.3, Addison-Wesley.
3. Ishan Wathuthanthri, Weidong Mao, and Chang-Hwan Choi, T*wo degrees-of-freedom* L*loyd-mirror interferometer for superior pattern coverage area*, Opt. Lett. **36**, No. 9, p. 1593 (May 1, 2011)
4. http://scienceworld.wolfram.com/physics/FringeVisibility.html
5. http://en.wikipedia.org/wiki/Interferometric_visibility
6. Hecht, reference 2 above, sections 12.2 and 14.3
7. Kyung Seok Cho, et al., I*mproved efficiency in GaAs solar cells by* 1D *and* 2D *nanopatterns fabricated by laser interference lithography*, Opt. Comm **10-11**, 2608, (15 May 2011)
8. M. Domanski, et al., N*ovel approach to produce nanopatterned titanium implants by combining nanoimprint lithography and reactive ion etching*, 14th International Conference on Miniaturized Systems for Chemistry and Life Sciences, 3-7 October 2010, Groningen, The Netherlands
9. G. Tizazu, et al., L*arge area nonpatterning of alkylphosphonate self-assembled monolayers on titanium oxide surfaces by interferometric lithography*, Nanoscale **3**, No. 6, p. 2511 (June 2011)
10. Ikjoo Byun and Joonwon Kim, C*ost-effective laser interference lithography using a* 405 *nm* AlI*n*G*a*N *semiconductor laser*, J. Micromech. Microeng. **20** 055204 (23 April 2010)
11. P. W. Wachuluk, et al., N*anopatterning in a compact setup using table top extreme ultraviolet lasers*, Opto-Electron. Rev. **16** No. 4, p. 444 (2008)
12. E. B. Hochberg and N. L. Chrien, http://hdl.handle.net/2014/26078 (June 8, 1996)
13. Christophe Martinez, et al., P*hase Plate Process for Advanced Fiber Bragg Gratings Devices Manufacturing*, IEICE Trans. Electron., **E83-C**, No. 3 (March 2000)
14. Takehiro Fukushima, et al., L*aser Diode Beam Shaping by Optical Interference*, Opt. Rev. **18**, No. 3, p. 287 (2011)
15. John Kielkopf and Lawrence Portaro, Appl. Optics, **31** No. 33, p. 7083 (1992)
16. H. Merdji, et al., C*oherence properties of high-order harmonics: Application to high-density laser-plasma diagnostics*, Laser and Particle Beams, **18**, p. 495 (2000)

Newport Corporation

Worldwide Headquarters
1791 Deere Avenue
Irvine, CA 92606

(In U.S.): 800-222-6440
Tel: 949-863-3144
Fax: 949-253-1680

Email: sales@newport.com

Newport
Experience | Solutions

Visit Newport Online at: **www.newport.com**

This Application Note has been prepared based on development activities and experiments conducted in Newport's Technology and Applications Center and the results associated therewith. Actual results may vary based on laboratory environment and setup conditions, the type and condition of actual components and instruments used and user skills.

Nothing contained in this Application Note shall constitute any representation or warranty by Newport, express or implied, regarding the information contained herein or the products or software described herein. Any and all representations, warranties and obligations of Newport with respect to its products and software shall be as set forth in Newport's terms and conditions of sale in effect at the time of sale or license of such products or software. Newport shall not be liable for any costs, damages and expenses whatsoever (including, without limitation, incidental, special and consequential damages) resulting from any use of or reliance on the information contained herein, whether based on warranty, contract, tort or any other legal theory, and whether or not Newport has been advised of the possibility of such damages.

Newport does not guarantee the availability of any products or software and reserves the right to discontinue or modify its products and software at any time. Users of the products or software described herein should refer to the User's Manual and other documentation accompanying such products or software at the time of sale or license for more detailed information regarding the handling, operation and use of such products or software, including but not limited to important safety precautions.

This Application Note shall not be copied, reproduced, distributed or published, in whole or in part, without the prior written consent of Newport Corporation.

Copyright ©2012 Newport Corporation. All Rights Reserved. The Newport "N" logo is a registered trademarks of Newport Corporation.